Contrib Mineral Petrol (1992) 112:414–427

Contributions to Mineralogy and Petrology
© Springer-Verlag 1992

A boundary layer-induced immiscibility in naturally re-equilibrated H_2O-CO_2-NaCl inclusions from metamorphic quartz (Western Carpathians, Czechoslovakia)

Vratislav Hurai[1]* and Elfrun-Erika Horn[2]

[1] Geochemisches Institut, Georg-August Universität, Goldschmidtstrasse 1, W-3400 Göttingen, FRG
[2] Institut für Geologie und Dynamik der Lithosphäre, Georg-August Universität, Goldschmidtstrasse 3, W-3400 Göttingen, FRG

Received October 4, 1991 / Accepted June 25, 1992

Abstract. Naturally re-equilibrated fluid inclusions have been found in quartz crystals from alpine fissures of the Western Carpathians. Re-equilibration textures, such as planar arrangement of the decrepitation clusters as well as the quartz c- and a-axis oriented fracturing indicate explosion of fluid inclusions. The extent of fracturing, which is dependent on inclusion diameters, suggests inclusion fluid overpressures between 0.6–1.9 kb. Microthermometry data are controversial with the textures because of indicating roughly fixed initial fluid composition and density during re-equilibration, although inclusion volumes have been sometimes substantially reduced by crystallization of newly-formed quartz. It is concluded that fluid loss from re-equilibrated inclusions must have been compensated for by replacing equivalent quartz volume from cracks into parent inclusions. Such a mechanism has operated in a closed system and the re-equilibration related cracks have not been connected with mineral surface. The compositional and density differences between aqueous inclusions in decrepitation clusters and CO_2-rich parent inclusions cannot be interpreted in terms of classical fluid immiscibility. Moreover, monophase liquid-filled aqueous inclusions and coexisting monophase CO_2 vapour-filled inclusions in the decrepitation clusters are thermodynamically unacceptable under equilibrium metamorphic conditions. The effect of disjoining pressure resulting from structural and electrostatic forces in very thin fractures is suspected to have caused density and compositional inconsistencies between parent and cluster inclusions, as well as the unusual appearance of cluster inclusions. In high-grade metamorphic conditions, the re-equilibration probably leads to boundary layer-induced immiscibility of homogeneous H_2O-CO_2-NaCl fluids and to formation of compositionally contrasting CO_2-rich and aqueous inclusions.

Correspondence to: V. Hurai

* *Permanent address:* Geological Institute, Comenius University, 84215 Bratislava, Czechoslovakia

Introduction

Lemmlein and Kliya (1954) were probably the first to describe naturally exploded fluid inclusions. Such inclusions were later recorded in impactite craters (e.g. Pagel and Poty 1975), in crustal and mantle xenoliths (e.g. De Vivo et al. 1988), in pegmatites (Voznyak and Kalyuzhniy 1976; Kalyuzhniy 1982) and most frequently in regionally metamorphosed rocks (Kreulen 1980; Swanenberg 1980; Crawford and Hollister 1986; Behr 1989 among others). The textures related to implosion as well as to the re-equilibration in a pressure stress field have been described in geological samples only very recently (Boullier et al. 1991; Hall et al. 1991).

The laboratory re-equilibration of fluid inclusions was first conducted at 1 atm confining P and various T to estimate the critical P gradient required for irreversible deformation and to test the decrepitation behaviour of inclusions in relation to their diameter and to the character of the host (Naumov et al. 1966; Khetchikov et al. 1968; Tugarinov and Naumov 1970; Leroy 1979; Gratier and Jenatton 1984; Bodnar et al. 1989). Another group of experiments was performed in autoclaves filled with fluid medium at elevated T and P to simulate isobaric cooling or isothermal decompression in metamorphic terraines (Pecher 1981; Pecher and Boullier 1984; Sterner and Bodnar 1989; Boullier et al. 1989; Bakker and Jansen 1991). The third group of experiments was carried out in an oriented P stress field induced by a solid medium apparatus (Pecher 1981; Gratier and Jenatton 1984).

The aim of this report is to show that textures incidental to the natural re-equilibration sometimes differ from those observed in the laboratory. Another aspect of this study is connected with reporting on the unusual chemical and physical properties of the fluids liberated from H_2O-CO_2 inclusions during re-equilibration. It will be documented too, that fluid densities preserved in the re-equilibrated inclusions are not in accordance with the large P differentials indicated by extensive fracturing and by recrystallization of inclusion walls.

Geological setting

The Alpine-Carpathian mountain belt was formed as a result of an intercontinental collision during the Miocene. The Veporicum tectonic unit located in the central part of the Western Carpathians (Fig. 1) seems to be exceptional, because available fission track (Král' 1977) and K/Ar data (Burchart et al. 1987; Hurai et al. 1991) indicate postmetamorphic uplift in the Upper Cretaceous. The Veporicum tectonic unit is the only in the Western Carpathians to have undergone a strong paleo-Alpine deformation accompanied by regional metamorphism under the conditions of chlorite to garnet zone of greenschist facies (Vrána 1966, 1980).

The Veporicum consists of the largest complexes of the metamorphites and intrusive granitic Hercynian bodies throughout the Western Carpathians. Metasedimentary sequences (Precambrian? monotonous high-grade gneisses and early-to-late Paleozoic low-to-medium grade graphitic, chloritic and sericitic schists, metabasaltic and metarhyolitic tuffs, marbles, dolomites and magnesites) can be subdivided into several units believed to be overthrust and folded during two Pre-Alpine (Hercynian?) and one Alpine (Cretaceous) deformation stages accompanied by regional metamorphism (Bezák 1988).

The fissures originated in the Upper Cretaceous during an extensional phase of the last metamorphic event as evidenced by:
1. Crystallization temperatures between 320–495 °C estimated from the K/Na ratios in the aqueous phase of inclusion fluids (Hurai and Stresko 1987)

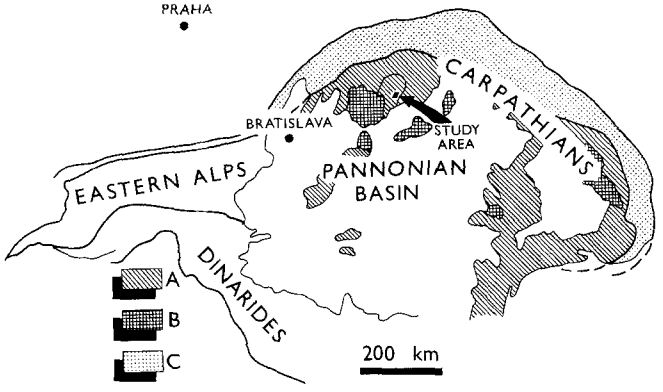

Fig. 1. Tectonic map of the Alpine-Carpathian region (roughly after Royden and Burchfiel 1989). *A*, pre-Tertiary complexes; *B*, Tertiary volcanics; *C* flysch sediments of the Outer Carpathians

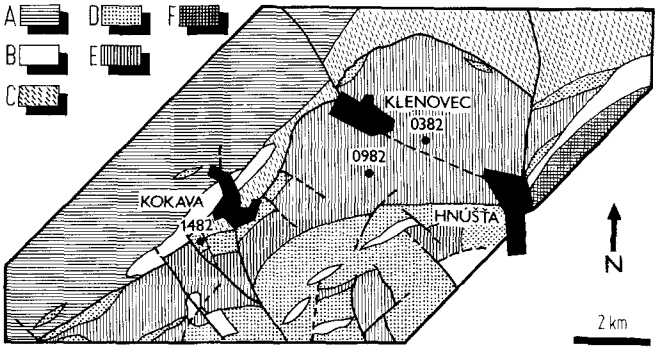

Fig. 2. Geological map of the area designated by arrow in Fig. 1 with *numbers* and *locations* of the samples used in this study (geological backround adapted from Bezák 1988). *A*, the Král'ova hol'a-complex (migmatites, hybrid granitoides); *B*, the Rimavica-complex (granitoides); *C*, the Ostrá-complex (garnet mica schists, amphibolites – early Paleozoic); *D*, the Sinec-complex (slates, metavolcanites, metaconglomerates, magnesites – late Paleozoic); *E*, the Klenovec-complex (albitized biotitic paragneisses – early Paleozoic); *F*, the Slatvina-formation (Carboniferous)

2. Formation pressures as high as 2.8–4.3 kb indicated by the densities of non re-equilibrated fluid inclusions in the central part of the Veporicum (Hurai, unpublished)
3. K/Ar model ages of the fissure adularia between 71–90 Ma (Hurai et al. 1991)
4. Lack of the deformation textures in fissure minerals
5. NE-SW direction of most fissures, i.e. parallel to the youngest tectonic elements in the Veporicum.

The euhedral fissure quartz containing re-equilibrated inclusions has been found at three localities in the southermost part of the Veporicum unit (Figs. 1, 2). The fissures represent the youngest formation stage characteristic of the circulation of CO_2-rich fluids along vertical fractures and sheared zones at temperatures between 320–420 °C. The fissures are located in metasedimentary host rocks of the middle structural stage (the Klenovec complex, sample nos. 0382, 0982) and of the upper structural stage (the Sinec complex, sample no. 1482). These complexes were deformed mainly during the youngest Alpine tectono-metamorphic events (Bezák 1988).

Analytical techniques

Fluid inclusions were studied in doubly polished plates on the CHAIXMECA freezing-heating stage calibrated by MERCK chemical standards as well as according to the melting point of distilled water (0 °C) and phase transitions in natural pure CO_2 inclusion with critical homogenization at 31.1 °C and triple point at −56.6 °C.

The empirical equations of Potter et al. (1978) and Bozzo et al. (1973) have been used for salinity calculations from *Tm* of ice or CO_2 clathrate. Isochores for CO_2-rich inclusions were derived according to the method of Burruss (1981) from the equations of state by Angus et al. (1976) and by Bowers and Helgeson (1983) using the computer algorithm by Nicholls and Crawford (1985). Isochores for aqueous fluids have been generated by computer program of Hurai (1989) based on the least square fit to the experimental data of Hilbert (1979) and Gehrig (1980).

Gas species in the vapour phase of inclusions and quartz characteristics have been studied by multichannel detector (PRINCETON INST. INC., 1024 diodes) coupled with RAMANOR U-1000 Raman microprobe (JOBIN-YVON). The exciting radiation – 514.5 nm green light – has been produced by 5 W ionized Ar^+ laser (COHERENT INNOVA-90). The power of the laser source was 700 or 2000 mW. Quantification of Raman data has been carried out using equations, procedures and factors described by Pasteris et al. (1988) and Dubessy et al. (1989).

Polished quartz plates covered with conductive graphite coating have been utilized for cathodoluminescence (CL) observations. The CL in the visible spectral range was excited by electron beam (12–15 kV, 0.5 mA) in an university-made instrument with "hot" cathode gun. The monochromatic CL images have been obtained on the same samples in the CAMBRIDGE INST. Ltd. scanning electron microscope under 20 kV voltage.

Microscopic description of the re-equilibration phenomena

Fracturing and recrystallization of re-equilibrated inclusions

Various re-equilibration stages can be illustrated on an example of Klenovec quartz (Fig. 3), in which the following deformation types have been classified in a group of coexisting inclusions:

ND-type inclusions (non-decrepitated) – the smallest intact inclusions without optically discernible fracturing and recrystallization (Fig. 3a)

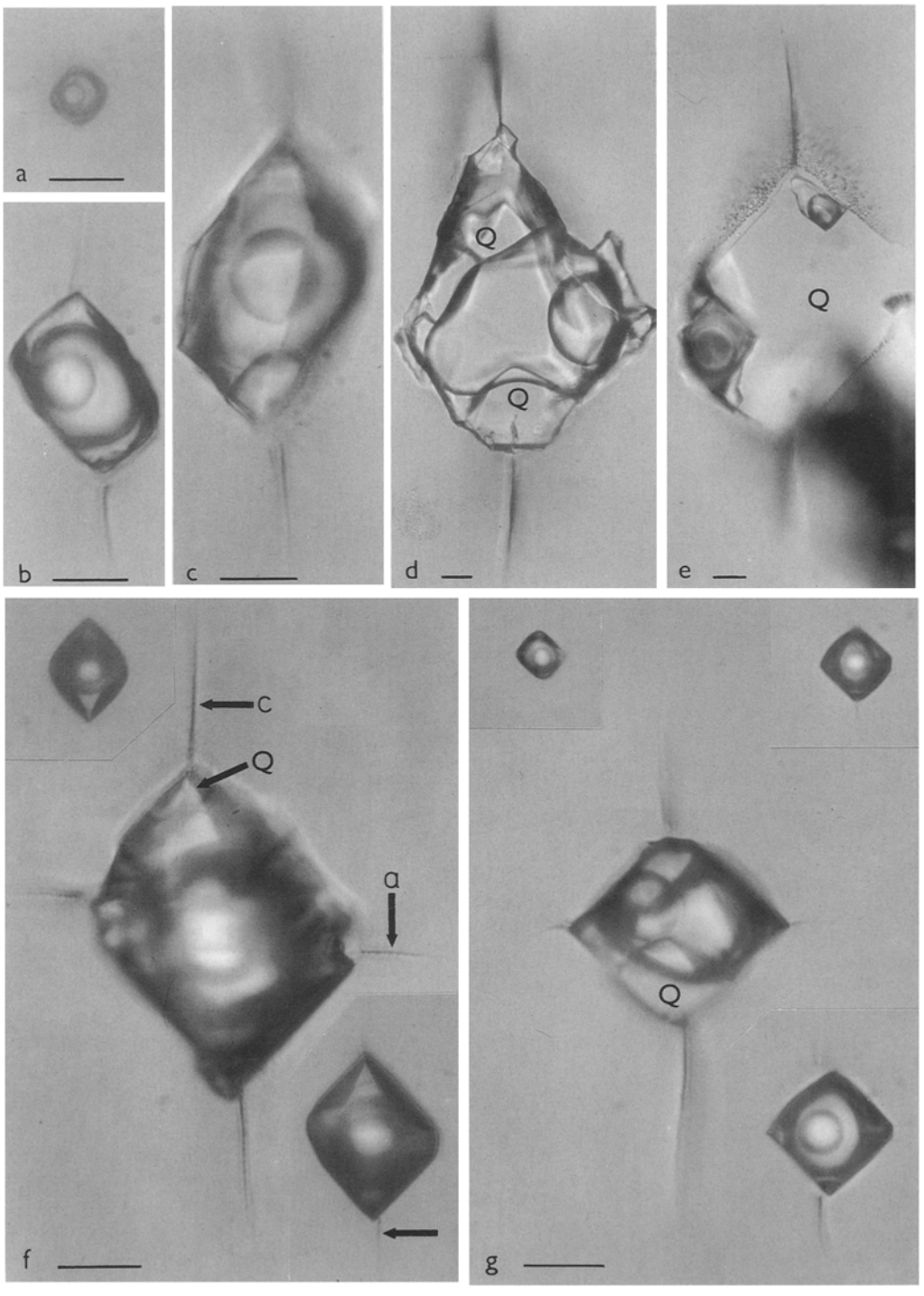

Fig. 3a–g. Various stages of fluid inclusion re-equilibration in the Klenovec quartz, sample 0982/I (**a–c**), 0382 (**f**), 0982/II (**g**). **a** ND-type inclusion without optically visible cracking; **b** D-type inclusion showing germinal stage of c-axis oriented fracturing and wall recrystallization; **c–e** DR-type recrystallized inclusions with various volumes of newly-formed quartz (*Q*). Scale bars represent 10 μm

D-type inclusions (decrepitated) – the inclusions exhibiting fracturing and initial stages of wall recrystallization (Fig. 3b)

DR-type inclusions (decrepitated and recrystallized) – the largest inclusions showing intensive fracturing and recrystallization accompanied by growing euhedral quartz on inclusion walls parallel to the c- and a-axes of the host (Fig. 3c–e).

As documented by a series of photomicrographs in Fig. 3, the intensity of fracturing and recrystallization depends on the inclusion diameter, the larger the inclusion, the more intensive re-equilibration phenomena. In the most advanced stage, the inclusion cavity becomes almost completely rehealed with newly-formed quartz. The inclusion fluid is left behind only in the corners of the original inclusion, the perimeter of which remains discernible due to the decoration of the secondary inclusions retrapped in decrepitation clusters (Fig. 3e). The fractures are most frequently oriented parallel to the quartz c-axis and to a lesser extent to the a-axis (Fig. 3f, g). The a-cracks are always shorter and they are sometimes missing around flat and irregularly shaped inclu-

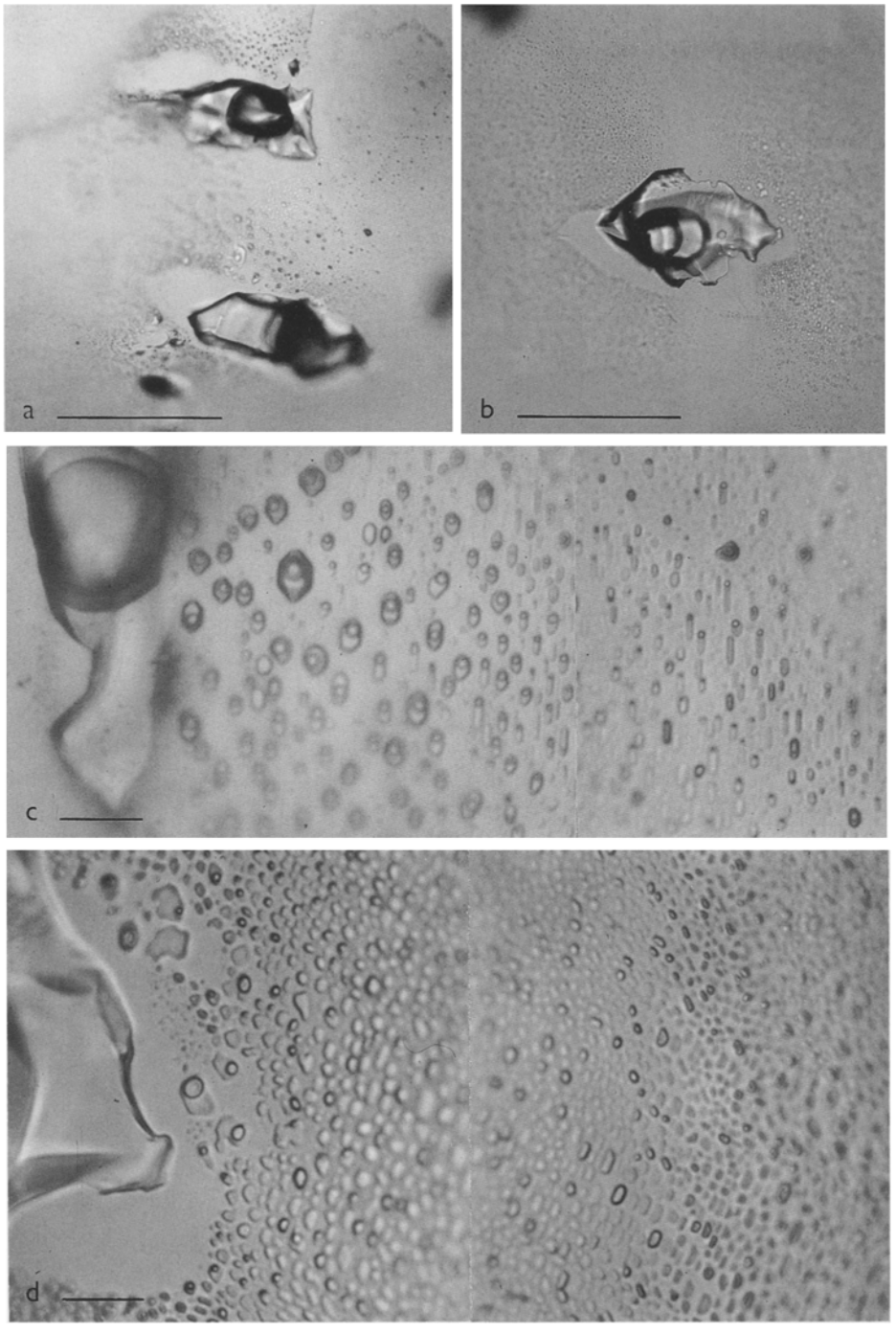

Fig. 4a–d. Decrepitation clusters around re-equilibrated inclusions in the Kokava (**a**, **c**) and Klenovec quartz (**b**, **d**). Illustrated are inclusion-free shadows (**a**, **b**) and anomalous appearance of cluster inclusions (**c**, **d**), in which volumetric phase ratios vary in dependence on the distance from the parent inclusion (see Table 1 for comparison). Note also the aqueous composition of the cluster inclusions and the CO_2-rich composition of the parent inclusions. Scale bars represent 100 μm in **a**, **b** and 10 μm in **c**, **d**

sions. The c-cracks are parallel to the edges of the rhombohedra $\{10\bar{1}1\}$ and join each other at an angle of 120° to form star-like arrays in the view along quartz c-axis in a similar manner to that described by Voznyak and Kalyuzhniy (1976), and Kalyuzhniy (1982) in naturally exploded inclusions from pegmatitic quartz.

Behaviour of inclusions in clusters

Re-equilibration related cracks are decorated by secondary inclusions which are optically almost invisible around negative crystal shaped inclusions and considerably larger around flattened, irregularly shaped inclusions. These decrepitation clusters sometimes contain specific inclusion-free shadows, the outer perimeter of which delineates precisely, from one side, the perimeter of re-equilibrated parent inclusions (Fig. 4a, b).

Another specific phenomenon is the compositional difference between re-equilibrated and the associated cluster inclusions. Although the re-equilibrated inclusions always contain CO_2 liquid phase at room T, in their clusters only monophase and two-phase aqueous

Table 1. Correlation between volumetric phase ratios and diameters of aqueous cluster inclusions in various distances from the re-equilibrated inclusion shown in Fig. 4c

Vol.% G	1–2 μm	2–3 μm	3–4 μm	4–5 μm	>5 μm	Σ
Distance 0–24 μm, 78 inclusions						
0–10	1.3%	1.3%	3.8%	3.8%	–	10.2%
10–25	–	15.4%	14.1%	29.5%	21.7%	80.7%
25–50	–	1.3%	2.6%	1.3%	–	5.2%
50–100	–	1.3%	1.3%	1.3%	–	3.9%
Σ	1.3%	19.3%	21.8%	35.9%	21.7%	100.0%
Distance 24–48 μm, 100 inclusions						
0–10	1.0%	13.0%	10.0%	3.0%	3.0%	30.0%
10–25.	1.0%	9.0%	17.0%	14.0%	12.0%	53.0%
25–50	1.0%	4.0%	4.0%	5.0%	2.0%	16.0%
50–100	–	–	1.0%	–	–	1.0%
Σ	3.0%	26.0%	32.0%	22.0%	17.0%	100.0%
Distance 48–72 μm, 146 inclusions						
0–10	5.5%	19.2%	30.9%	3.4%	–	59.0%
10–25.	0.7%	3.4%	19.9%	8.2%	–	32.2%
25–50	–	1.3%	4.1%	2.1%	–	7.5%
50–100	–	–	1.3%	–	–	1.3%
Σ	6.2%	23.9%	56.2%	13.7%	–	100.0%
Distance 72–105 μm, 170 inclusions						
0–10	9.4%	35.3%	17.6%	0.6%	–	62.9%
10–25.	–	2.9%	13.5%	1.2%	–	17.6%
25–50	–	1.8%	9.4%	0.6%	–	11.8%
50–100	0.6%	2.4%	4.7%		–	7.7%
Σ	10.0%	42.4%	45.2%	2.4%	–	100.0%

inclusions have been observed (Fig. 4c, d). The only two-phase aqueous inclusions have been recorded in newly-formed quartz growing inside the re-equilibrated inclusions.

Table 1 correlates the diameters of cluster inclusions in Fig. 4c with their liquid-to-vapour ratios in four distance categories from the parent inclusion. Apart from documenting the wedged shape of the cluster with smallest inclusions on its periphery, some correlation of the volumetric phase ratios with inclusion positions is also indicated. Two-phase aqueous inclusions with 10–25 vol.% of vapour prevail close to the parent inclusion, whereas the distribution pattern in the outermost part of the cluster indicates the predominance of high-density inclusions with up to 10 vol.% of vapour. The percentage of high-density, and especially monophase inclusions, increases systematically in the four selected distance categories (<24 μm, 24–48 μm, 48–72 μm and 72–105 μm) in sequence as follows: 10, 30, 59, and 63%. In a similar manner, the number of vapour-dominated, low-density inclusions also tends to increase towards the external part of the cluster, so that the ratio of low-density/high-density inclusions in outermost part of the cluster (8:63, i.e. 13:100) compares well with the vapour-to-liquid phase ratios (from 10:100 to 25:100) of the most individual inclusions close to the parent inclusion.

The same phenomenon for the Klenovec quartz is documented in Fig. 4d. The cluster inclusions have clearly reached a lower maturation degree (usage of this term in the sense of Bodnar et al. 1985) in comparison with well maturated, negative crystal-shaped inclusions in the Kokava quartz. Variable phase ratios involving G-dominated and monophase L-filled inclusions are visible close to the parent inclusion, while merely monophase G-filled and monophase L-filled inclusions are present in the external part of the cluster. Planimetric point analysis has shown that 63% of the cluster area, in its external part, is composed of fluid inclusions and that vapour occupies 15% of the total fluid volume. Similarly, 60% of the cluster area in the part close to parent inclusion is occupied by fluid inclusions and 17% of the total fluid volume is represented by vapour. It may be thus concluded that despite large variations in the vapour-to-liquid ratios of individual inclusions throughout the cluster, the bulk fluid density remains fixed.

Raman and cathodoluminescence study on quartz

The presumed structural differences between the host and the newly-formed quartz have been checked by Raman records and by cathodoluminescence (CL) images. The vibrational Raman spectra of both quartz types were identical and yielded only the peaks characteristic of low (α) modification.

No different cathodoluminescence has been observed in the visible spectral range and both quartz types dis-

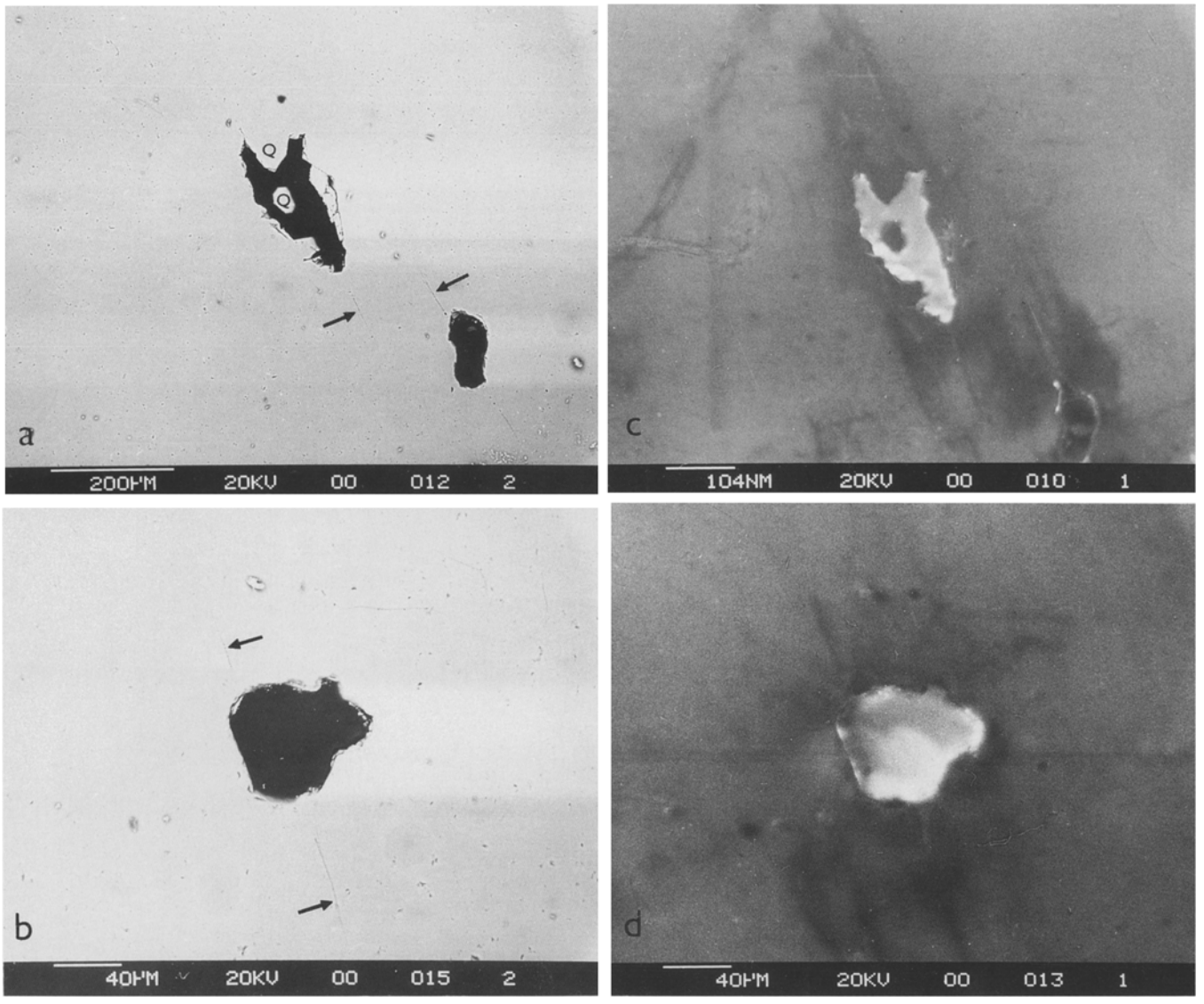

Fig. 5a, b. Back scattered electron and **c, d** cathodoluminescence images of DR-type inclusions showing microscopically visible c-oriented cracks (*arrows*) and newly-formed quartz (*Q*) in **a, b**, and optically invisible haloes delineating inclusion shapes in **c, d**

played the same blue colour, believed to be typical of plutonic, volcanic and medium-to-high grade metamorphic quartz (Marshall 1988).

On the other hand, the SEM-CL images have revealed specific haloes otherwise invisible under a polarizing microscope (Fig. 5). The haloes following the outer perimeter of inclusions occurred only around DR-type inclusions. Their presence might be attributed to a higher OH^- content and/or to optically invisible arrays of water-rich inclusion fluids, expelled from the parent inclusions during explosion (Behr 1989).

Fluid inclusion data

In all of the samples studied, CO_2 densities and CO_2 contents of fluid inclusions decrease more less steadily from earliest to latest inclusion planes and the re-equilibration phenomena are confined only to the oldest CO_2-rich inclusions. Table 2 shows this scenario for the Klenovec quartz example, in which the relative ages of inclusions were possible to determine by observation of intersecting planes. The earliest systems (i.e. groups of primary, or planes of pseudosecondary and secondary inclusions) are placed on the top of Table 2, the latest are at the bottom.

No signs of a heterogeneous trapping have been observed and possible formation PT conditions are thus defined by corresponding isochores in the one-phase region. Isochoric projection in Fig. 6 shows that trapping conditions of re-equilibrated inclusions (black areas) mostly do not overlap the PT envelopes for younger CO_2-rich and aqueous inclusions.

It should be mentioned that microthermometry has been complicated by decrepitation of the CO_2-rich inclusions on heating. The density and compositional data have been inferred from the volume of carbonic phase at room T using the procedure proposed by Burruss

Table 2. Microthermometry data on re-equilibrated and intact inclusions from Klenovec quartz

	Tm ice (°C)	Tm hydr. (°C)	Salinity (% NaCl eq.)	Th CO_2 (°C)	CO_2 (vol.%)	Th (°C)	Density (g/cc)	CO_2 (mol.%)	H_2O (mol.%)
Sample 0982/I									
System									
A[a]	−4.1 to −5.4	7.9–9.5	1.0–4.1	28.9–29.8 (L)	40–50	–	0.803–0.868	14.2–20.6	78.3–84.9
A	–	7.4–7.9	4.1–4.5	29.1–29.8 (L)	40–50	–	0.817–0.870	14.2–20.5	78.5–84.7
C[a]	–	8.9–9.0	2.0–2.2	30.9–31.1 (G)	60–65	–	0.615–0.684	22.3–23.5	76.0–77.1
C	–	9.0	2.0	31.0–31.1 (G)	60–65	–	0.627–0.683	22.3–24.3	75.2–77.2
B	–	9.0–9.5	1.0–2.0	30.6–31.1 (L)	55–60	–	0.681–0.763	22.0–22.3	77.4–77.5
D	−8.0 to −10.0	–	11.7–14.0	–	–	198–221	0.936–0.977	–	–
Sample 0982/II									
System									
A[a]	−5.3	8.5–8.6	2.8–3.0	27.6–28.9 (L)	50–55	–	0.806–0.841	21.4–24.1	75.2–77.8
A	–	8.3–8.6	2.8–3.4	28.1–28.9 (L)	50–55	–	0.806–0.837	21.2–24.1	75.2–78.0
H[a]	−5.4	7.5–8.6	2.8–4.9	27.1–28.1 (L)	60–65	–	0.781–0.818	29.4–33.3	66.1–69.5
H	–	7.5–8.5	3.0–4.9	28.0–28.1 (L)	60–65	–	0.781–0.806	28.7–33.3	65.6–70.6
E[a]	−5.1	7.8	4.3	30.7–30.9 (G)	60–65	–	0.598–0.640	19.1–21.9	77.0–79.8
E	−5.7	7.8–8.4	3.2–4.3	30.9 (G)	60–65	–	0.618–0.652	19.9–23.5	75.4–79.3
C	–	9.0–9.6	0.8–2.0	30.4–30.8 (G)	70–75	–	0.522–0.577	27.3–30.9	68.9–72.2
B, D	–	8.5–9.8	0.4–3.0	31.1 (crit.)	65–70	–	0.626–0.659	26.2–30.9	69.0–73.1
F, I	–	9.0–9.9	0.2–2.0	30.7–31.0 (L)	60–70	–	0.658–0.736	25.5–33.0	67.0–74.1
J	–	9.2–9.6	0.8–1.6	30.9 (G)	65–70	–	0.544–0.614	23.5–25.0	74.8–76.1
G	−7.6 to −9.4	3.9–4.3	~10–12	–	20–30	225–240	0.911–0.945	–	–
K	−11.0 to −11.3	–	15.0–15.4	–	–	180–206	0.978–1.006	–	–
L	Monophase aqueous inclusions								

[a] Re-equilibrated inclusions

Table 3. Microthermometry data on neighbouring ND (intact), D (decrepitated) and DR (decrepitated and recrystallized) inclusions from Klenovec quartz

Sample	System	Type	Tm CO_2 (°C)	Tm hydr. (°C)	Salinity (% NaCl eq.)	Th CO_2 (°C)	CO_2 (vol.%)
No. 0982/I	A	ND	−57.0	7.9	4.1	29.2 (L)	40–50
		D	−57.0	7.9	4.1	29.4 (L)	40–50
		DR	−56.8	8.5	3.0	29.1 (L)	40–50
		ND	−56.7	7.9	4.1	29.8 (L)	40–50
		D	−56.7	8.2	3.6	29.1 (L)	40–50
		DR	−56.7	8.3	3.4	28.9 (L)	40–50
		ND	−56.9	7.4	5.1	29.5 (L)	40–50
		DR	−56.9	8.3	3.4	29.1 (L)	40–50
		ND	−56.6	7.8	4.3	29.1 (L)	40–50
		DR	−56.7	8.3	3.4	28.9 (L)	40–50
No. 0982/II	A	ND	−56.6	8.3	3.4	28.8 (L)	50–55
		DR	−56.5	8.6	2.8	28.6 (L)	50–55
	H	ND	−57.1	–	–	28.1 (L)	60–65
		D	−57.1	8.5	3.0	28.0 (L)	60–65
		DR	−57.1	7.6	4.7	27.8 (L)	60–65
		D	−56.6	7.5	4.9	28.0 (L)	60–65
		DR	−56.6	8.6	2.8	27.5 (L)	60–65
	E	ND	−56.6	7.8	4.3	30.9 (G)	60–65
		D	−56.6	8.4	3.2	30.8 (G)	60–65
No. 0382	B	ND	−56.8	6.8	6.1	30.1 (L)	25–30
		D	−56.8	7.2	5.4	30.1 (L)	25–30
	C	ND	−56.7	7.4	5.1	29.6 (L)	30–35
		D	−56.7	7.7	4.5	29.5 (L)	30–35
		DR	−56.7	7.9	4.1	29.6 (L)	30–35

(1981). Such an approach may lead to errors in the case of strongly recrystallized, irregularly shaped DR-type inclusions. To overcome this problem and to check possible density variations between various inclusion types, the temperatures of CO_2 homogenization versus inclusion diameters have been correlated in various systems containing re-equilibrated inclusions (Fig. 7).

The results show that despite pressure differentials of 0.6–1.9 kb inferred from the minimum diameter of D-type inclusions, the CO_2 densities remain fixed. In

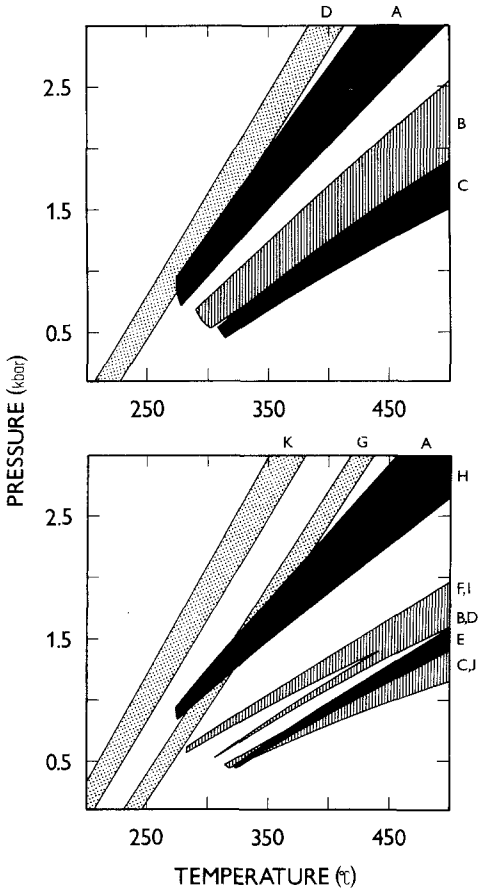

Fig. 6. Isochoric *P T* projection of microthermometry data on Klenovec quartz (Table 2). *Solid areas*, isochores for re-equilibrated CO_2-rich inclusions, *dashed areas*, isochores for later planes of CO_2-rich intact inclusions, *dotted areas*, isochores for secondary aqueous inclusions

some cases (sample 0982/I – system A, sample 0982/II – systems A and H) even slightly increased CO_2 density in the D- and DR-type inclusions has been recorded.

This trend is illustrated more distinctly in Table 3, where the microthermometric data on the neighbouring inclusions only have been selected. It is also shown that in nine of the ten cases documented, the salinity of the aqueous phase in re-equilibrated inclusions is lower than in the intact inclusions.

Table 4 summarizes available microthermometry data for re-equilibrated parent inclusions and coexisting cluster inclusions. In two cases, the inclusion data in the newly-formed quartz have been estimated. In seven of the eight cases documented, salinities of the aqueous inclusions in the clusters and in the newly-formed quartz are from 2.2 to 6.9 wt.% NaCl eq. higher than those in parent CO_2-rich inclusions.

Although clathrate formation, CO_2-liquid condensation and/or phase transitions around the CO_2 triple point have not been noticed on cooling the cluster inclusions, the presence of CO_2 in their vapour phase has been confirmed by Raman spectra. The depression of Tm_{ice} is, however, greater than -1.5 °C, i.e. the maximum of Tm_{ice} depression in the binary system H_2O-CO_2 without the presence of CO_2 clathrate (Hedenquist and Henley 1985), and thus the greater portion of the solutes present must be represented by dissolved salts.

Discussion

The compositional inconsistency between cluster and parent inclusions is one of the most striking problems of this study. Of particular importance is, which fluid, the aqueous in clusters or the carbonic in parent inclusions, is representative of the initial fluid composition prior to onset of re-equilibration. The second question to be answered is whether both compositionally different fluids can represent coexisting phases.

The presence of CO_2 in the coexisting intact and re-equilibrated inclusions suggests that the CO_2 is the representative component of the original fluid and that initial composition has at least partly been preserved during re-equilibration. The aqueous composition of the cluster inclusions might suggest their identity with the fluid surrounding quartz crystals during re-equilibration. The following reasons, however, invalidate such an assumption:

1. Aqueous fluids comparable with those in cluster inclusions have not been found to form individual secondary trails, not being intimately associated with re-equili-

Table 4. Microthermometry data on re-equilibrated CO_2-rich and coexisting aqueous cluster inclusions

Locality	Sample	Re-equilibrated parent inclusions						Coexisting cluster inclusions		
		Tm CO_2 (°C)	Tm ice (°C)	Tm hydr. (°C)	Th CO_2 (°C)	CO_2 (vol.%)	Salinity (% NaCl eq.)	Tm ice (°C)	Th (°C)	Salinity (% NaCl eq.)
Kokava	No. 1482	−57.0[a]	−4.6	8.4	29.3 (G)	30	3.2	−3.3	–	5.4
		−57.0[a]	–	8.3	29.4 (G)	30	3.4	−3.5	–	5.7
		−57.1[a]	−4.5	9.2	28.8 (G)	30	1.6	−3.5	–	5.7
Klenovec	No. 0382	−56.7	−6.1	8.2	30.1 (L)	35	3.6	−0.8; −1.0	163; 188	1.4; 1.7
		−56.9	−4.0	9.5	30.1 (G)	35	1.0	−3.9; −5.0	227; 212	6.3; 7.9
		−56.7	−5.1	9.1	29.2 (G)	35	1.8	−4.7[b]	185	7.4
Klenovec	No. 0982/I	−56.6	–	9.5	29.4 (L)	50	1.0	−3.8[b]	214	6.1
		−56.7	−5.1	8.4	29.0 (L)	50	3.2	−4.3	191	6.9

[a] Depression of $TmCO_2$ due to presence of 4–8 mol.% N2
[b] Aqueous inclusions in newly-formed quartz

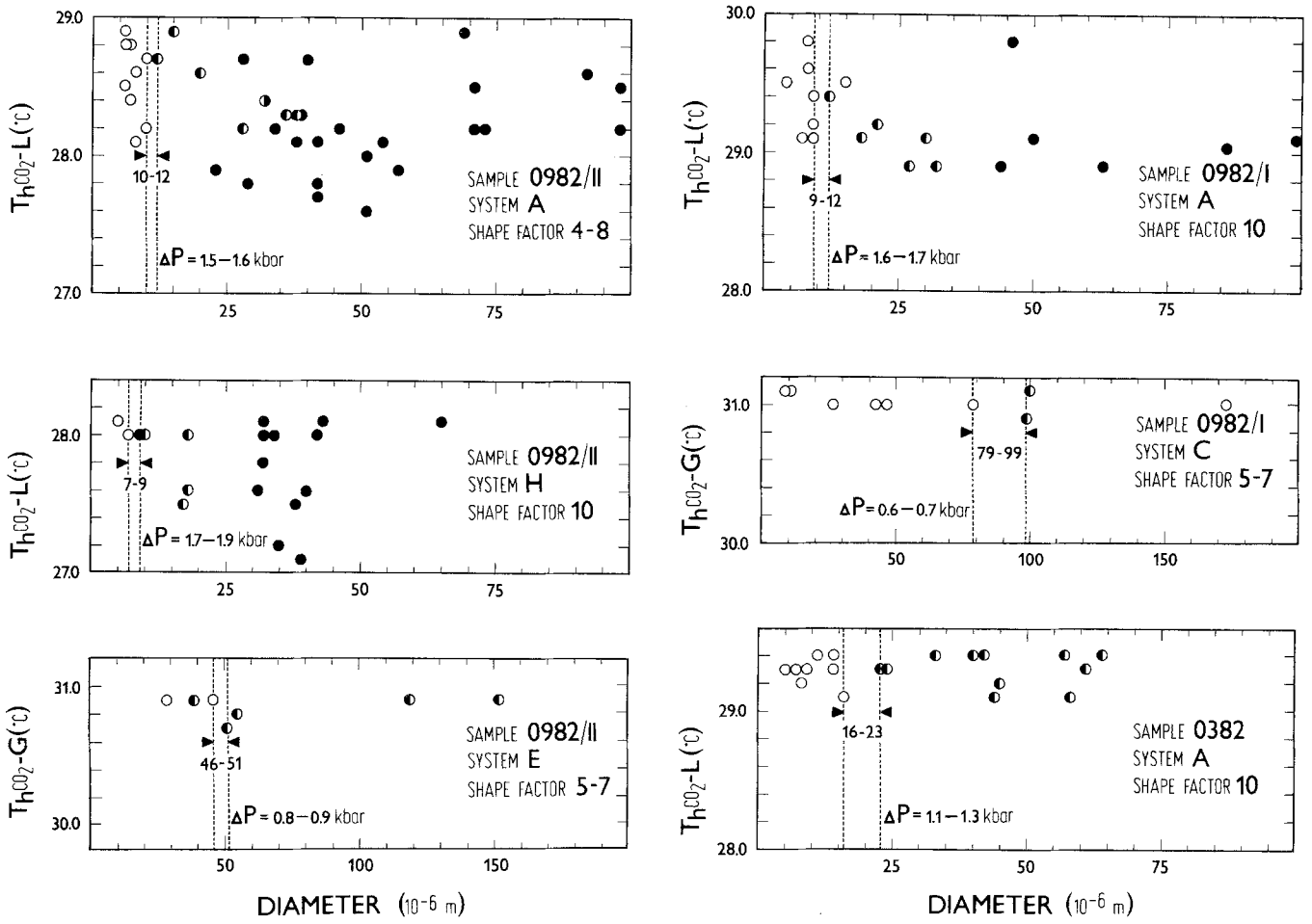

Fig. 7. Diagrams correlating inclusion diameters with partial homogenization of CO_2-rich phase. *Open circles*, intact inclusions, *solid circles*, DR-type inclusions, *combined circles*, D-type inclusions. *ΔP* represents critical inclusion overpressure required to cause explosion calculated from the equation by Bodnar et al. (1989)

brated inclusions (compare, for instance, entirely different salinities of the secondary aqueous inclusions in the system D, sample no. 0982/I, Table 2, and cluster inclusions from the same sample in Table 4).

2. Original CO_2-rich solutions have not been completely drawn out of the parent inclusions.

3. NaCl concentrations in the re-equilibrated inclusions are generally lower than that in the neighbouring intact inclusions (Table 3). Since the cluster inclusions have higher salinity than their parent inclusions (Table 4), this effect can have been caused only by a loss of the aqueous phase of the higher salinity.

There are thus several serious reasons to claim that aqueous fluids in clusters and CO_2-rich fluids in parent inclusions can represent coexisting phases separated during re-equilibration.

Theoretical modelling

An attempt has been made to reconstruct volume and compositional changes during re-equilibration from available microthermometry data. The average values from the system A, sample no. 0982/I (Table 3) have served as input data for the following scenario. An intact CO_2-rich inclusion containing 4.4 wt.% NaCl, with partial $Th(\rightarrow L)CO_2$ at 29.4 °C and with 40 vol.% of the carbonic phase at this temperature, has undergone a re-equilibration during which the salinity decreased from 4.4 to 3.3 wt.% NaCl and the partial *Th* of CO_2 liquid has dropped from 29.4 to 29.0 °C. The released aqueous phase retrapped in clusters contained 6.9 wt.% NaCl (Table 4) and a negligibly small amount of CO_2.

The mass balance calculations in this section are based on the principles outlined by Bodnar (1983) and Bodnar et al. (1985). The intact inclusion contains 84.33 mol.% H_2O, 14.46 mol.% CO_2 and 1.19 mol.% NaCl and its bulk density is 0.8632 g/cm^3. A total of 1000 cm^3 of the initial fluid contains theoretically 589.35 g H_2O, 246.9 g CO_2 and 26.98 g NaCl. From this solution, a total of 30.56 wt.% of the aqueous phase with 6.9% NaCl must be liberated to yield the remainder CO_2-rich fluid with 3.3 wt.% NaCl. The mass of the released solution is 188.35 g, i.e. 175.35 g H_2O plus 13 g NaCl. The remainder solution now contains 414 g H_2O, 246.9 g CO_2 and 13.98 g NaCl (79.71 mol.% H_2O, 19.46 mol.% CO_2 and 0.83 mol.% NaCl). If the initial volume of the inclusion were preserved, the bulk density would decrease to 0.6749 g/cm^3 as a result of the liberation of the aqueous fluid. At a room temperature of

20 °C, such an re-equilibrated inclusion would contain 58.1 vol.% of the carbonic phase with partial $Th(\rightarrow G)$ at 31.0 °C. This is, however, not in agreement with microthermometry data which indicate higher CO_2 density (Table 3, Fig. 7). If the composition were fixed, the CO_2 density increase could have been caused merely by the 19% reduction of inclusion volume and concomitant bulk density increase from 0.6749 g/cm^3 to 0.8308 g/cm^3. At 20 °C, such a modified inclusion now contains 48.4 vol.% of the carbonic phase (36.2 vol.% of CO_2 liquid and 12.2 vol.% of CO_2 vapour) which is in good agreement with the visual observations and microthermometry data.

The density of the released $H_2O+NaCl$ fluid should reach 0.8631 g/cm^3. This value was obtained by dividing the mass of released $H_2O+NaCl$ solution (188.35 g) by the volume difference between the initial bulk density (0.8632 g/cm^3) and the density after liberation of the $H_2O+NaCl$ phase (0.6749 g/cm^3). The density of the released aqueous phase corresponds to $Th=201$ °C which compares with Th in cluster inclusions. The volume changes calculated are graphically depicted in Fig. 8.

Although the mass balance calculations in the preceding paragraphs are in accord with the fluid properties in the re-equilibrated inclusions and their clusters, they do not agree with experimental phase equilibria in the system H_2O-CO_2-NaCl. The model discussed supposes the existence of the two immiscible fluids, one water-rich with 6.9 wt.% NaCl wetting the inclusion walls and one CO_2-rich with 4.4 wt.% NaCl not being attached to the inclusion walls.

According to Roedder and Bodnar (1980) and Pichavant et al. (1982), coexisting immiscible phases trapped in separate inclusions should possess the following characteristics:

1. Homogenization of the water-rich phase occurs in L and the coexisting CO_2-rich phase homogenizes to G.

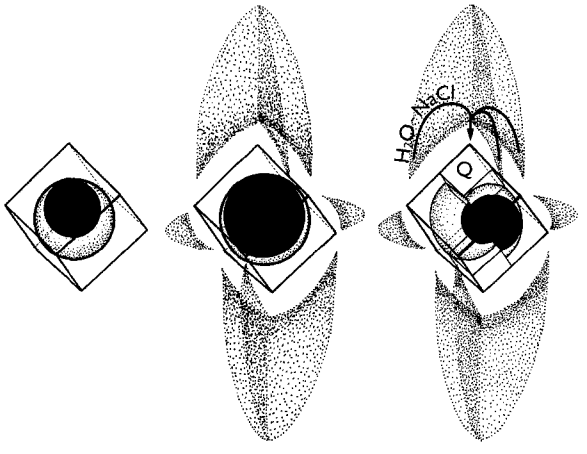

Fig. 8. Hypothetical volume and compositional changes in a negative crystal shaped intact inclusion (*left*) after onset of fracturing accompanied by expulsion of aqueous phase (*middle*) and after precipitation of newly formed quartz *Q* (*right*), based on the mass balance calculations in this study. The shape of inclusion and the orientation of cracks have been taken from Voznyak and Kalyuzhniy (1976)

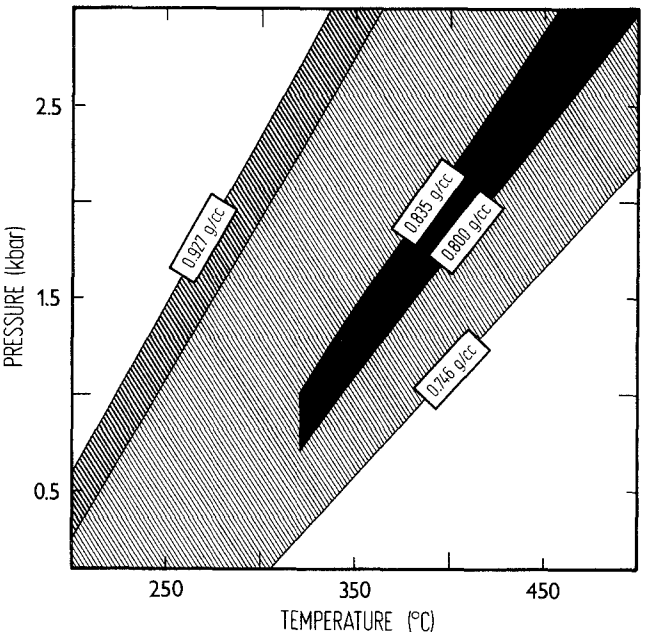

Fig. 9. Isochoric PT projection of microthermometric data from the plane of inclusions illustrated in Fig. 4a. *Dashed areas*, isochores for aqueous cluster inclusions, *solid area*, isochores for CO_2-rich parent inclusions. Isochores for 90% of the cluster inclusions pass through the PT box expressed by *heavy lines* in the *dashed area*

2. Th are equal to or higher than trapping temperatures.
3. In the PT plane, respective isochores must intersect each other in the point corresponding to the trapping conditions.

Two of these criteria are not fulfilled in our model because the respective isochores of parent and cluster inclusions do not intersect each other and as discussed later, the re-equilibration temperature cannot correspond to the Th of cluster inclusions.

At 200 °C, the internal pressure in the CO_2-rich intact inclusion reaches only 500–600 bar which is too low to cause the explosion even of the largest inclusions in the system, not taking into account the internal overpressure of 1.6–1.7 kb indicated by diameters of re-equilibrated inclusions (Fig. 7). Moreover, at 200 °C and 500 bar, the water-rich liquid phase in the immiscibility region of the system H_2O-CO_2-NaCl still contains a significant amount of carbon dioxide. Using the data of Takenouchi and Kennedy (1965), as much as 7.2 wt.% of CO_2 should be dissolved in CO_2-saturated $H_2O+6\%$ NaCl solution at these PT conditions. This concentration is high enough to be detected on cooling with help of microthermometry methods. Contrary to this, no phase transitions in the examined cluster inclusions around −56.6 °C indicate that the CO_2 density is below that in triple point (0.0139 g/cm^3, Angus et al. 1976) and that the bulk CO_2 concentration is even lower than in the case of the sealing water-rich phase at room temperature along three-phase $L_{H_2O}L_{CO_2}G_{CO_2}$ boundary.

A similar discrepancy was also recorded in the Kokava quartz where two-phase cluster inclusions homogenize to L between 165–301 °C with a maximum frequency

of between 165–186 °C. The *Th* of CO_2-rich parent inclusions falls within the range of 320–322 °C. As shown in Fig. 9, isochores of cluster inclusions with lowest *Tm* do not intersect the isochores for parent inclusions and do not thus comply with the criteria for immiscible coexisting fluid phases.

Explosion or implosion?

As discussed in the preceding section, microthermometry data indicate that water-rich phase has been expelled out of inclusions during re-equilibration. This phenomenon, however, cannot be used as evidence for explosion, because Bakker and Jansen (1991) have documented that such a mechanism may operate also during implosion.

It has to be emphasized that most of the textural phenomena observed in the samples studied indicate re-equilibration under conditions of inclusion fluid overpressure:

1. Quartz c-axis oriented fracturing and planar shape of the decrepitation clusters.
2. Haloes around DR-type inclusions displayed in SEM/CL images.
3. Intensity of fracturing tending to increasing proportionally with inclusion diameter. The opposite are true in cases of implosion (Thomas 1990, personal communication; Hall et al. 1991).

On the other hand, the collapse of inclusion cavities and their elimination by newly-formed quartz would favour the concept of the inclusion fluid underpressure during re-equilibration. Although Pecher and Boullier (1984), and Bodnar et al. (1989) have reported similar explosion-related recrystallization, the volume conserving dissolution-precipitation mechanism advanced by them to account for this phenomenon cannot be accepted for the situation here. The mechanism has been found to operate only within elongated or flattened inclusions possessing high surface free energy. In our case, the arrays of microfracturing and coeval intact inclusions indicate that the DR-type inclusions originally had energetically stable negative crystal shapes (Fig. 3).

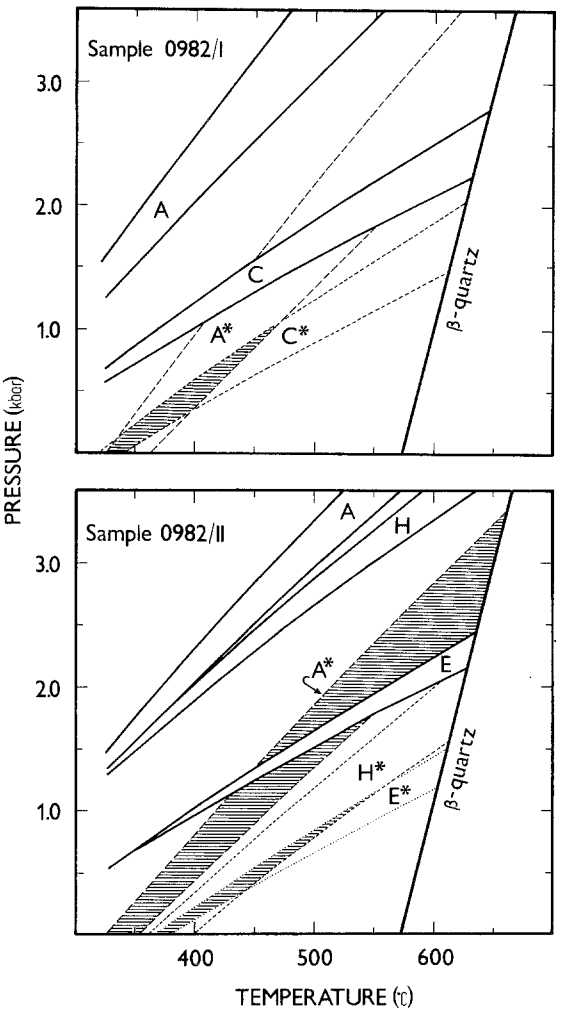

Fig. 10. Re-equilibration *PT* conditions (*dashed areas*) for Klenovec quartz derived from isochores of intact inclusions (Table 2) and from minimum diameter of coexisting re-equilibrated inclusions. *Asterisks* designate apparent isochores for re-equilibrated inclusions obtained by subtracting ΔP (Fig. 7) from the isochores for intact inclusions. The boundary of quartz $\alpha-\beta$ transition has been calculated according to Koster van Groos and Ter Heege (1973)

Controversy of fluid densities

The other puzzling problem of this study stems from the fact that inclusion densities have been maintained during re-equilibration, although minimum diameters of re-equilibrated inclusions indicate internal overpressures between 0.6–1.9 kb (Fig. 7). Moreover, inclusion density and composition seems to be nearly unchanged even if about 80 vol.% of the cavity has been filled by newly-formed quartz (Fig. 3e). Such observations are contrary to experimental studies which have always recorded a more or less simple evolution of inclusion densities toward the values corresponding to *PT* conditions of re-equilibration (e.g. Pecher and Boullier 1984; Sterner and Bodnar 1989).

The inconsistency between textural and fluid inclusion data can be documented for the example of Klenovec quartz (Fig. 10). Re-equilibration *PT* conditions (dashed areas) have been derived from the isochores of intact inclusions (designated A, C, E, H) by subtracting the inclusion overpressure (ΔP) calculated from the minimum diameter of D-type inclusions (Fig. 7) according to the equation given by Bodnar et al. (1989). The actual isochores for D- and DR-type inclusions do not pass through the re-equilibration *PT* conditions estimated, even if possible error bands, resulting from the uncertainty in the visual estimation of volumetric phase ratios, are taken into account. Such a controversy might be explained by the following mechanisms:

1. *Explosion has been followed by reset of confining PT conditions to the same values as the trapping PT conditions.* This mechanism can be rejected, because significant density differences exist between individual systems of re-equilibrated inclusions. It is very unlikely that each system should have undergone re-equilibration under

entirely different PT conditions and after each event, the original trapping PT conditions of the individual group of inclusions could have been restored.

2. *All inclusions, including those with diameters below 5 μm, have been re-equilibrated to new PT conditions.* Considering the negative crystal shape of the inclusions, the fluid overpressures must have then attained about 2.5 kb and the isochores appropriate to the original fluids would project unreasonably high PT conditions inconsistent with mineralogical and geological data. Moreover, there is no reason why the re-equilibration related cracks should be optically invisible around inclusions with diameter up to 79 μm (system C, sample 0982/I) although they are clearly discernible around 12 μm inclusions occurring in another system from the same sample (Fig. 7).

It can be concluded that quartz is able to compensate fluid loss from re-equilibrating inclusions by displacing the equivalent volume of the silica from cluster into parent inclusions, thus maintaining the initial inclusion density. The cause of such a behaviour remains, however, unknown.

Boundary layer effect

The unusual appearance of the cluster inclusions is the last phenomenon, which merits special attention, because it cannot be satisfactorily explained with help of commonly accepted mechanisms of fluid inclusion formation.

The coexistence of monophase aqueous liquid inclusions and inclusions with varying liquid/vapour ratios is usually interpreted as a result of post-trapping modifications due to recrystallization (necking-down) at temperatures below 100 °C (Roedder 1984; Bodnar et al. 1985). Behaviour of the cluster inclusions is, however, just opposite to that expected from this model, because well equilibrated negative crystal shaped inclusions tend to possess uniform liquid/vapour ratios (Fig. 4c), while immature flattened inclusions with a higher recrystallization potential exhibit inconsistent volumetric ratios (Fig. 4d). Merely monophase liquid and monophase vapour inclusions shown in Fig. 4d cannot result from necking-down, because such a process must lead to the formation of two-phase inclusions with intermediate bulk densities. These conclusions are not substantially modified by the fact that the monophase L-filled inclusions are probably metastable stretched inclusions which have failed to nucleate a small volume percentage of a vapour bubble due to small dimensions (Roedder 1984, p. 296), and that a thin liquid film may have been overlooked in the vapour inclusions with diameters below 3 μm.

The phenomena observed in cluster inclusions might be perhaps attributed to the effect of disjoining pressure, which is believed to be created by van der Waals structural forces and an electrostatic double layer in fluid films wetting the charged silicate surfaces. The disjoining P does not depend on the magnitude of hydrostatic P in coexisting bulk fluid (Deryagin and Churaev 1986; Belonoshko and Schmulovich 1986). The magnitude of structural and electrostatic components of the disjoining P change in unequal extent across a distance from the solid surface. For instance at room T, the water layer attached to the quartz surface may develop electrostatic β-films up to 0.3 μm thick with lifetimes only several hours, and stable α-films up to 0.06 μm thick, primarily determined by structural forces. The negative disjoining P is created in the distances between 0.007–0.06 μm due to predominance of electrostatic attraction over the forces of structural repulsion. The maximum P in the β-films is reached at a distance of 0.1 μm from the quartz surface. The disjoining P in the α-films is considerably higher and may attain several tens kilobars at distances below 0.004 μm (Deryagin and Churaev 1986). The existence of high disjoining P at geologically important PT conditions has been evidenced by molecular dynamic simulations (Belonoshko and Schmulovich 1987; Belonoshko 1988). Direct observations of fluid properties in wetting films have often yielded ambiguous results, but there is no doubt that solid surfaces influence the properties of attached fluids at distances below 0.05 μm. This effect is multiplied in two-dimensional cracks and one-dimensional capillaries (Clifford 1975).

The effect of disjoining P may perhaps account for unusual phase ratios in cluster inclusions, inside which surface forces might have acted on polar water and non-polar CO_2 molecules to an unequal extent causing the density variations observed in aqueous inclusions, while the CO_2-rich phase has remained intact preserving its low density throughout the whole cluster. It seems, however, very improbable that the effect of disjoining P can be observed optically (Belonoshko and Schmulovich 1987). On the other hand, the initial thickness of the re-equilibration related cracks must have been considerably lower than actually observed dimensions of the cluster inclusions. For example, Shelton and Orville (1980) have obtained three-dimensional inclusions 5–10 μm in size by healing a 0.1–0.2 μm thick fracture.

It seems to be plausible that surface forces strongly attack fluids entering re-equilibration related cracks, mainly in the crack tips, and that these forces can cause compositional and density differences between the crack and bulk fluids in polycomponent systems. Such an effect has been simulated for H_2O-CO_2 fluids by Belonoshko (1989) who has shown that capillary fluids must be depleted in CO_2 with respect to the bulk fluid within a broad range of PT conditions beyond classical immiscibility limits postulated for the system H_2O-CO_2. Thus, it seems to be reasonable that when the re-equilibration related crack recedes due to recrystallization, isolated islands of unhealed crack may conserve non-equilibrium fluid properties, thus creating density and compositional inconsistencies in a manner described in this study.

The concept of the anomalous fluid properties in submicrometer spaces may account for the last controversy, the massive quartz recrystallization inward re-equilibrated inclusions. Experimentally evidenced negligible solubility of quartz in hydrothermal solutions would suggest that large fluid volumes must have circulated through re-equilibrated inclusions to produce the large volumes

of newly-formed quartz. Contrary to this, the original fluid seems to be preserved during re-equilibration and the volume of newly-formed quartz is also dependent on the inclusion diameter (as shown in Fig. 3), quartz recrystallization occurs only in the largest re-equilibrated inclusions.

Experimental works have shown that water condensed in very thin quartz capillaries may extract as much as 2–37% silica from the capillary walls due to high corrosivity caused by structural protonization (Spitsyn et al. 1972). Such highly concentrated, melt-resembling aqueous solutions are stable only in submicrometer volumes and when entering macroscopic spaces, they disintegrate by precipitating large amounts of dissolved components (Ershova and Churaev 1977).

A similar effect is suspected to operate in the re-equilibrated inclusions. The volume of newly-formed quartz is very probably proportional to the volume of the attached crack, which is primarily controlled by inclusion diameters. Moreover, such a mechanism corroborates fluid inclusion and textural data indicating that the re-equilibration has taken place in a closed system and that the re-equilibration related cracks have not reached the surface of the quartz host.

Conclusions

Sterner and Bodnar (1989) have concluded that most fluid inclusions in metamorphic minerals cannot withstand, without a re-equilibration, the large differentials between internal inclusion pressure and confining pressure during postmetamorphic evolution of PT conditions. A preferred strain-induced leakage of water from CO_2-rich aqueous inclusions has been envisaged in high-grade metamorphic conditions by Hollister (1990) to account for pure CO_2 inclusions controversial with the mineral equilibria suggestive of high water activity.

It seems likely that modifications of initially mixed H_2O+CO_2 inclusions due to the re-equilibration accompanied by the boundary-layer induced immiscibility is not uncommon in metamorphic conditions. Compositionally contrasting H_2O and CO_2 fluids originating in such a way may be retrapped in individual inclusion planes even in micrometer distances. As a result of the surface forces and the concomitant additional disjoining pressure, developed in submicrometer spaces independently from the magnitude of the bulk fluid pressure, both crack confined and coexisting bulk fluid exhibit compositional and density differences which are not interpretable in terms of classical experimental fluid systems.

Acknowledgements. We would like to thank Edwin Roedder, Jacques Touret, Alfons van den Kerkhof, and an anonymous reviewer for their thoughtful critiques and review of this paper. We are also grateful to Stefan Gerschütz and Alfons van den Kerkhof for cathodoluminescence records, and especially, Klaus Simon and Markus Pohlmann for providing computing facilities. Stimulating discussion with Rainer Thomas is also gratefully acknowledged. Financial support from the Alexander von Humboldt Foundation for the first author enabled this work to be done.

References

Angus S, Armstrong B, De Reuck KM (1976) International thermodynamic tables of the fluid state, carbon dioxide. Pergamon, New York, pp 1–67

Bakker RJ, Jansen JBH (1991) Experimental post-entrapment water loss from synthetic CO_2-H_2O inclusions in natural quartz. Geochim Cosmochim Acta 55:2215–2230

Behr HJ (1989) Die geologische Aktivität von Krustenfluiden. Nds Akad Geowiss Veröfftl 1:7–42

Belonoshko AB (1988) Molecular dynamics modelling of water on the β-quartz surface (in Russian). Zh Fizi Khim 62, 1:118–121

Belonoshko AB (1989) The thermodynamics of the aqueous carbon dioxide fluid within thin pores. Geochim Cosmochim Acta 53:2581–2590

Belonoshko AB, Shmulovich KI (1986) A study of dense fluid in micropores by molecular dynamics technique (in Russian). Geokhimiya 11:1523–1534

Belonoshko AB, Schmulovich KI (1987) Fluid phase in fine pores at high pressures (in Russian). Dokl Akad Nauk SSSR – Phys Chem 295, 3:625–629

Bezák V (1988) Tectonic development of the south-western part of Veporicum, West Carpathians (in Slovak). Mineralia Slovaca 20, 2:131–142

Bodnar RJ (1983) A method of calculating fluid inclusion volumes based on vapor bubble diameters and P-V-T-X properties of inclusion fluids. Econ Geol 78:535–542

Bodnar RJ, Binns PR, Hall DL (1989) Synthetic fluid inclusions. VI. Quantitative evaluation of the decrepitation behaviour of fluid inclusions in quartz at one atmosphere confining pressure. J Metam Geol 7:229–242

Bodnar RJ, Reynolds TJ, Kuehn CA (1985) Fluid inclusion systematics in epithermal systems. In: Berger BR, Bethke PM (eds) Geology and geochemistry of epithermal systems. Rev Econ Geol 2:73–97

Boullier AM, France-Lanord C, Dubessy J, Adamy J, Champenois M (1991) Linked fluid and tectonic evolution in the High Himalaya Mountains (Nepal). Contrib Mineral Petrol 107:358–372

Boullier AM, Michot G, Pecher A, Barres O (1989) Diffusion and/or plastic deformation around fluid inclusions in synthetic quartz: new investigations. In: Bridgwater D (ed) Fluid movements – element transport and the composition of the deep crust. NATO ASI Series 281. Kluwer, Dordrecht, pp 345–360

Bowers TS, Helgeson HC (1983) Calculation of the thermodynamic and geochemical consequences of nonideal mixing in the system H_2O-CO_2-NaCl on phase relations in geologic systems: equation of state for H_2O-CO_2-NaCl fluids at high pressures and temperatures. Geochim Cosmochim Acta 47:1247–1275

Bozzo AT, Chen JR, Barduhn AJ (1973) The properties of the hydrates of chlorine and carbon dioxide. In: Delyannis A, Delyannis E (eds) 4th International symposium on fresh water from sea, vol 3, Heidelberg, pp 437–451

Burchart J, Cambel B, Král' J (1987) Isochron reassessment of K–Ar dating from the West Carpathian crystalline complexes. Geol Zborn Geolog Carpath 38:131–170

Burruss RC (1981) Analysis of fluid inclusions: phase equilibria at constant volume. Am J Sci 281:1104–1126

Clifford J (1975) Properties of water in capillaries and thin films. In: Franks F (ed) Water – a comprehensive treatise, vol 5. Plenum Press, New York London, pp 75–132

Crawford ML, Hollister LS (1986) Metamorphic fluids: The evidence from fluid inclusions. In: Walther JV, Wood BJ (eds) Fluid-rock interactions during metamorphism. Springer, New York Berlin Heidelberg, pp 1–35

Deryagin BV, Churaev NV (1986) Properties of water layers adjacent to interfaces. In: Croxton CA (ed) Fluid interfacial phenomena. Wiley, New York, pp 663–738

De Vivo B, Frezzotti ML, Trigila R (1988) Spinel lehrzolite nodules from Oahu island (Hawaii): a fluid inclusion study. Bull Minéral 111:307–319

Dubessy J, Poty B, Ramboz C (1989) Advances in C-O-H-N-S fluid geochemistry based on micro-Raman spectrometric analysis of fluid inclusions. Eur J Mineral 1:517–534

Ershova GF, Churaev IV (1977) IR-absorption spectra of water in thin layers between quartz slides (in Russian). Kolloidn Zh 39:1151–1154

Gehrig M (1980) Phasengleichgewichte und pVT-Daten ternären Mischungen aus Wasser, Kohlendioxid und Natriumchlorid bis 3 kbar und 550 °C. Dr rer nat Dissertation, Hochschulverlag, Freiburg, pp 1–109

Gratier JP, Jenatton L (1984) Deformation by solution-deposition, and re-equilibration of fluid inclusions in crystals depending on temperature, internal pressure and stress. J Structural Geol 6:189–200

Hall DL, Bodnar RJ, Craig JR (1991) Fluid inclusion constraints on the uplift history of the metamorphosed massive sulphide deposits at Ducktown, Tennessee. J Metam Geol 9:551–565

Hedenquist JW, Henley RW (1985) The importance of CO_2 on freezing point measurements of fluid inclusions: evidence from active geothermal systems and implications for epithermal ore deposition. Econ Geol 80:1379–1406

Hilbert R (1979) pVT-Daten von Wasser und von wäßrigen Natriumchlorid-Lösungen bis 873 K, 4000 Bar und 25 Gewichtsprozent NaCl. Dr-Ing Dissertation, Hochschulverlag, Freiburg, pp 1–212

Hollister LS (1990) Enrichment of CO_2 in fluid inclusions in quartz by removal of H_2O during crystal-plastic deformation. J Structural Geol 12:895–901

Hurai V (1989) BASIC program for interpretation of microthermometric data from H_2O and $H_2O-NaCl$ fluid inclusions. Comput Geosci 15:135–142

Hurai V, Dávidová S, Kantor J (1991) Adularia from alpine fissures of the Veporicum crystalline complexes: morphology, physical and chemical properties, fluid inclusions and K/Ar dating (in Slovak). Mineralia Slovaca 23:133–144

Hurai V, Stresko V (1987) Correlation between quartz crystal morphology and composition of fluid inclusions as inferred from fissures in central Slovakia (Czechoslovakia). Chem Geol 61:225–239

Kalyuzhniy A (1982) Principles of knowledge about mineral-forming fluids (in Russian). Naukova Dumka, Kiev, pp 1–240

Khetchikov LN, Dorogovich BA, Samoylovich LA (1968) Dependence of corrections to homogenization temperatures and of decrepitation of gas-liquid inclusions in minerals on pressure, density and composition of fluids, on example of quartz (in Russian). Geol Rud Mestorozhd 3:87–97

Král' J (1977) Fission track ages of apatites from some granitoid rocks in West Carpathians. Geol Zborn Geolog Carpath 28:269–276

Koster van Groos AF, Ter Heege JP (1973) The high-low quartz transition up to 10 kilobars pressure. J Geol 81:717–723

Kreulen R (1980) CO_2-rich inclusions during regional metamorphism on Naxos (Greece): Carbon isotopes and fluid inclusions. Am J Sci 280:745–771

Lemmlein GG, Kliya MO (1954) The alteration of liquid inclusions under influence of host crystal overheating (in Russian). Dokl Akad Nauk SSSR – Geol 94, 2:233–236

Leroy J (1979) Contribution à l'étalonnage de la pression interne des inclusions fluides lors de leur décrépitation. Bull Minéral 102:584–593

Naumov VB, Balitskiy VS, Khetchikov LN (1966) Correlation of the temperatures of formation, homogenization and decrepitation of gas-liquid inclusions (in Russian). Dokl Akad Nauk SSSR – Geol 171:146–148

Marshall DJ (1988) Cathodoluminescence of geologic materials. Unwin Hyman, Boston, pp 1–146

Nicholls J, Crawford ML (1985) FORTRAN programs for calculation of fluid properties from microthermometric data on fluid inclusions. Comput Geosci 11:619–645

Pagel M, Poty B (1975) Fluid inclusion studies in rocks of the Charlevoix structure (Quebec, Canada). Fortschr Mineral 52 (Spec Iss):479–489

Pasteris JD, Wopenka B, Seitz JC (1988) Practical aspects of quantitative laser Raman microprobe spectroscopy for the study of fluid inclusions. Geochim Cosmochim Acta 52:979–988

Pecher A (1981) Experimental decrepitation and re-equilibration of fluid inclusions in synthetic quartz. Tectonophysics 78:567–583

Pecher A, Boullier AM (1984) Evolution à pression et temperature élevées d'inclusions fluids dans un quartz synthétic. Bull Minéral 107:139–153

Pichavant M, Ramboz C, Weisbrod A (1982) Fluid immiscibility in natural processes: use and misuse of fluid inclusion data. Chem Geol 37:1–27

Potter RW, Clyne MA, Brown DL (1978) Freezing point depression of aqueous sodium chloride solutions. Econ Geol 73:284–285

Roedder E (1984) Fluid inclusions. Mineral Soc Am Rev Mineral, vol 12:1–644

Roedder E, Bodnar RJ (1980) Geologic pressure determination from fluid inclusion studies. Earth Planet Sci Ann Rev 8:263–301

Royden R, Burchfiel BC (1989) Are systematic variations in thrust belt style related to plate boundary processes? (The Western Alps versus the Carpathians). Tectonics 8:51–61

Shelton KL, Orville PM (1980) Formation of synthetic fluid inclusions in natural quartz. Am Mineralogist 65:1233–1236

Spitsyn VI, Glazunov MP, Mulyar VM, Deryagin BV, Churaev NV, Zorin ZM (1972) A neutron activation analysis of anomalous water (in Russian). Dokl Akad Nauk SSSR – Phys Chem 202, 1:132–135

Sterner SM, Bodnar RJ (1989) Synthetic fluid inclusions. VII. Re-equilibration of fluid inclusions in quartz during laboratory-simulated metamorphic burial and uplift. J Metam Geol 7:243–260

Swanenberg HEC (1980) Fluid inclusions in high-grade metamorphic rocks from S.W. Norway. Geol Ultraiectina, vol 25, Utrecht, pp 1–147

Takenouchi S, Kennedy GC (1965) The solubility of carbon dioxide in NaCl solutions at high temperatures and pressures. Am J Sci 263:445–454

Tugarinov AI, Naumov VB (1970) Dependence of the decrepitation temperature of minerals on the composition of their gas-liquid inclusions and hardness (in Russian). Dokl Akad Nauk SSSR – Geol 195:112–114

Voznyak DK, Kalyuzhniy VA (1976) Utilization of decrepitated inclusions for reconstruction of PT conditions of mineral formation [on example of pegmatitic quartz from Volyn] (in Russian). Mineral Sb 30:31–40

Vrána S (1966) Alpinische Metamorphose der Granitoide und der Foederata-Serie im Mittelteil der Veporiden. Sb Geol Ved Záp Karpaty 6:29–84

Vrána S (1980) Newly-formed Alpine garnets in metagranitoids of the Veporides in relation to the structure of the Central zone of the West Carpathians. Cas Mineral Geol 25:41–54

Editorial responsibility: J. Hoefs